NAVAL POSTGRADUATE SCHOOL

MONTEREY, CALIFORNIA

THESIS

COMMUNICATIONS SYSTEM DESIGN LEVERAGING MULTIPLE RECEIVERS

by

Konstantinos Chorozoglou

June 2023

Thesis Advisor: Frank E. Kragh
Co-Advisor: Ralph C. Robertson

THIS PAGE INTENTIONALLY LEFT BLANK

REPORT DOCUMENTATION PAGE	*Form Approved OMB No. 0704-0188*

1. AGENCY USE ONLY *(Leave blank)*	**2. REPORT DATE** June 2023	**3. REPORT TYPE AND DATES COVERED** Master's thesis

4. TITLE AND SUBTITLE
COMMUNICATIONS SYSTEM DESIGN LEVERAGING MULTIPLE RECEIVERS

5. FUNDING NUMBERS

6. AUTHOR(S) Konstantinos Chorozoglou

7. PERFORMING ORGANIZATION NAME(S) AND ADDRESS(ES)
Naval Postgraduate School
Monterey, CA 93943-5000

8. PERFORMING ORGANIZATION REPORT NUMBER

9. SPONSORING / MONITORING AGENCY NAME(S) AND ADDRESS(ES)
N/A

10. SPONSORING / MONITORING AGENCY REPORT NUMBER

11. SUPPLEMENTARY NOTES The views expressed in this thesis are those of the author and do not reflect the official policy or position of the Department of Defense or the U.S. Government.

12a. DISTRIBUTION / AVAILABILITY STATEMENT
Approved for public release. Distribution is unlimited.

12b. DISTRIBUTION CODE
A

13. ABSTRACT (maximum 200 words)

In this thesis, we explore the potential advantages of collecting more received signal power through the use of multiple radios. A software radio is designed along with algorithms to combine the signals from multiple radios to allow reception of a signal in situations where it would be impossible with a single radio due to insufficient received power. Three techniques are explored to combine signals at different stages of decision-making. The first technique involves combining signals before calculating a single decision statistic. The second technique focuses on combining signals after calculating multiple branch statistics, leading to a composite symbol decision. Lastly, the third technique examines combining signals after multiple branch symbol decisions have been made. This may be of benefit in situations where increased range, covertness, or many small antennas are preferred to a single large antenna.

14. SUBJECT TERMS
software radio, receiver design, multiple receivers, improve SNR, improve Eb/N0, increase distance of communications

15. NUMBER OF PAGES
69

16. PRICE CODE

17. SECURITY CLASSIFICATION OF REPORT	**18. SECURITY CLASSIFICATION OF THIS PAGE**	**19. SECURITY CLASSIFICATION OF ABSTRACT**	**20. LIMITATION OF ABSTRACT**
Unclassified	Unclassified	Unclassified	UU

NSN 7540-01-280-5500

Standard Form 298 (Rev. 2-89)
Prescribed by ANSI Std. 239-18

THIS PAGE INTENTIONALLY LEFT BLANK

Approved for public release. Distribution is unlimited.

COMMUNICATIONS SYSTEM DESIGN LEVERAGING MULTIPLE RECEIVERS

Konstantinos Chorozoglou
Ipopliarhos, Hellenic Navy
Hellenic Naval Academy, 2009

Submitted in partial fulfillment of the
requirements for the degree of

MASTER OF SCIENCE IN ELECTRICAL ENGINEERING

from the

NAVAL POSTGRADUATE SCHOOL
June 2023

Approved by: Frank E. Kragh
Advisor

Ralph C. Robertson
Co-Advisor

Douglas J. Fouts
Chair, Department of Electrical and Computer Engineering

THIS PAGE INTENTIONALLY LEFT BLANK

ABSTRACT

In this thesis, we explore the potential advantages of collecting more received signal power through the use of multiple radios. A software radio is designed along with algorithms to combine the signals from multiple radios to allow reception of a signal in situations where it would be impossible with a single radio due to insufficient received power. Three techniques are explored to combine signals at different stages of decision-making. The first technique involves combining signals before calculating a single decision statistic. The second technique focuses on combining signals after calculating multiple branch statistics, leading to a composite symbol decision. Lastly, the third technique examines combining signals after multiple branch symbol decisions have been made. This may be of benefit in situations where increased range, covertness, or many small antennas are preferred to a single large antenna.

THIS PAGE INTENTIONALLY LEFT BLANK

TABLE OF CONTENTS

THIS PAGE INTENTIONALLY LEFT BLANK

LIST OF FIGURES

THIS PAGE INTENTIONALLY LEFT BLANK

LIST OF TABLES

THIS PAGE INTENTIONALLY LEFT BLANK

LIST OF ACRONYMS AND ABBREVIATIONS

ADC	Analog-to-Digital Conversion
BER	Bit Error Rate
I	In-Phase
ISI	Intersymbol Interference
MF	Matched Filter
MIMO	Multiple-Input Multiple-Output
SDR	Software Defined Radio
SNR	Signal-to-Noise Ratio
Q	Quadrature
QPSK	Quadrature-Phase Shift Keying

THIS PAGE INTENTIONALLY LEFT BLANK

I. INTRODUCTION

In this thesis, we explore three ways of leveraging multiple receivers for improving the performance of digital communications. In this chapter, we describe the research context, outline the current state of the topic and problems that may exist in this field, and then give a quick overview of previous related research as well as the major findings of these investigations. Finally, the problem formulation and the thesis outline are elaborated.

A. MOTIVATION – POSSIBLE APPLICATIONS

Multiple-receiver systems are increasingly popular in communication applications. The basic idea behind these systems is to use multiple receivers, or antennas, to collect a signal and then process it in some way to extract useful information. With multiple receivers, the system can collect more signal power than it can with a single receiver, which can be useful in situations where the signal is weak or noisy [1], [2].

There are many applications of multiple-receiver systems, ranging from military communication systems to civilian cell phone networks [1]–[3]. One important application is in the area of low-power communication. In some situations, it may be necessary to transmit signals at very low-power levels to avoid detection. In such cases, a multiple-receiver system can be used to collect and combine the weak signals from multiple receivers, thereby increasing the overall signal power and improving the chances of successful communication [1]–[3].

Another important application of multiple-receiver systems is in the area of long-distance communication. In some situations, it may be necessary to communicate over long distances, where the received signal strength is very weak. A single large gain antenna could solve the problem of collecting sufficient signal power, but sometimes that option is not available. For example, groups of mobile vehicles or individuals cannot carry a large dish antenna. Also, the ship to shore data rate to Navy ships could be substantially improved with greater aperture area, but the installation of a single larger aperture antenna is often inconsistent with warship operations. The installation of many small aperture antennas, however, may be more feasible for the above-mentioned groups or ships. By

using multiple receivers, it is possible to collect the weak signals from different receivers and combine them to form a stronger signal. Gathering the weak signals from various receivers can be particularly useful in situations where it is not possible to use a high-power transmitter, such as in remote areas or on a battlefield or where the propagation loss is huge, such as in satellite communication [2], [3].

In military applications, multiple-receiver systems can also be used to improve communication in situations where soldiers are dispersed over a wide area. For example, a platoon of soldiers may be spread out over the battlefield, which makes it difficult to maintain communication with the headquarters. By using multiple radios, it is possible to form an ad hoc array [4] and combine the signals from different radios to improve overall signal strength and reliability.

In addition to military applications, multiple-receiver systems can also be used in civilian applications. For example, in the case of cell phone networks, it is possible to use multiple cell phones to form an ad hoc array and improve signal reception in areas where coverage is weak [5]. This idea could be particularly useful for people traveling in a car or in remote areas where cell phone coverage is poor.

B. PRIOR RESEARCH AND KEY RESULTS

Generally, there has been a great deal of earlier study on different approaches in improving wireless communication systems, such as using several receivers to improve signal detection and transmission [1]–[3]. However, more work remains to be done to investigate the potential of these strategies in many settings and maximize their performance utilizing innovative technologies and algorithms.

Although the capabilities of leveraging multiple receivers are very promising in the field of exceptionally low signal-to-noise ratio (SNR) communications, there is a scarcity of literature reporting the results of such study in comparison to other techniques [1]–[3]. This may be true because the other methods also give satisfactory results.

A literature search on multiple receivers usually returns results related to Multiple-Input Multiple-Output (MIMO) systems. MIMO is a wireless communication antenna

system that employs multiple antennas at both the transmitter and the receiver [6]. These systems rely on channel fading, which is a phenomenon caused by multipath propagation. Channel fading is a phenomenon in which signals reflect on obstacles, such as buildings, resulting in signal attenuation and interference. Various approaches have been developed in MIMO systems to counteract the effects of channel fading and increase system performance [6], but this is not the topic of this research. While this thesis focuses on the use of multiple receivers, it ignores channel fading.

One paper with a similar topic to the subject of this thesis is a paper written by Y. V. Andreyev [2]. The author concentrates on systems that leverage multiple receivers for ultra-wideband communications. A model that uses an N-element transmitting and an N-element receiving system that increase the signal-to-noise ratio by a factor of N^2 is presented in this paper. Another interesting article with a similar topic was written by A. Singh, M. R. Bhatnagar, and R. K. Mallik [1]. Here, the authors investigate a multiple antennas system that performs cooperative spectrum sensing.

Another area that needs to be studied is software defined radio (SDR). Many books and articles have been written about this topic. SDR is a term that refers to radio systems in which most of the signal processing is conducted through software [7], and in this research the signal was generated and processed through MATLAB scripts and functions.

The development of SDR has led to the development of highly flexible and adaptable communication systems. One of the key advantages of SDR-based communication systems is their ability to combine signals from multiple receivers to increase SNR and improve communication reliability. This idea is elaborated in [8] where the creation of a virtual antenna by cooperative relaying is discussed.

C. RESEARCH QUESTION

There are several techniques for combining the signals from multiple receivers. One approach is to combine the individual signals before calculating a single composite decision statistic. Another approach is to combine the individual branch random variables before making a single composite symbol decision. A third approach is to combine the individual symbol decisions from each branch receiver to form a single composite symbol

decision. In this thesis, we seek to answer how these three types of receivers could be implemented, and how the overall performance of the system could be influenced by the multiple receivers.

D. CONCLUSION AND THESIS OUTLINE

In conclusion, multiple-receiver systems have a wide range of applications in both military and civilian settings. By using multiple receivers, it is possible to collect more signal power than with a single receiver, which can be useful in situations where the signal is weak or noisy. There are several different techniques for combining the signals from multiple receivers, each with its own advantages and disadvantages. As communication technology continues to evolve, it is likely that multiple-receiver systems will become even more important in enabling effective communication in a wide range of settings.

This thesis consists of five chapters. In Chapter II, we present important concepts in digital communications. Next, in Chapter III, we describe the design of the radios that were used for this research. In Chapter IV, the research outcome is analyzed, and various conclusions are drawn. Finally, in Chapter V, we provide the findings of this research and suggest areas for future research on this topic.

II. BACKGROUND KNOWLEDGE

In this chapter, we present communications theory. The information presented is very useful for the reader to understand the experiments conducted. We briefly cover the transmitter, channel, and receiver used in digital communications. Moreover, in this chapter we thoroughly cover signal-to-noise ratio (SNR) and E_b/N_0, white Gaussian noise, and the probability of error in quadrature phase-shift keying (QPSK). The information listed here has been drawn mainly from [9]–[11].

A. TRANSMITTER

A rough representation of a transmitter using the QPSK modulation technique is shown in Figure 1.

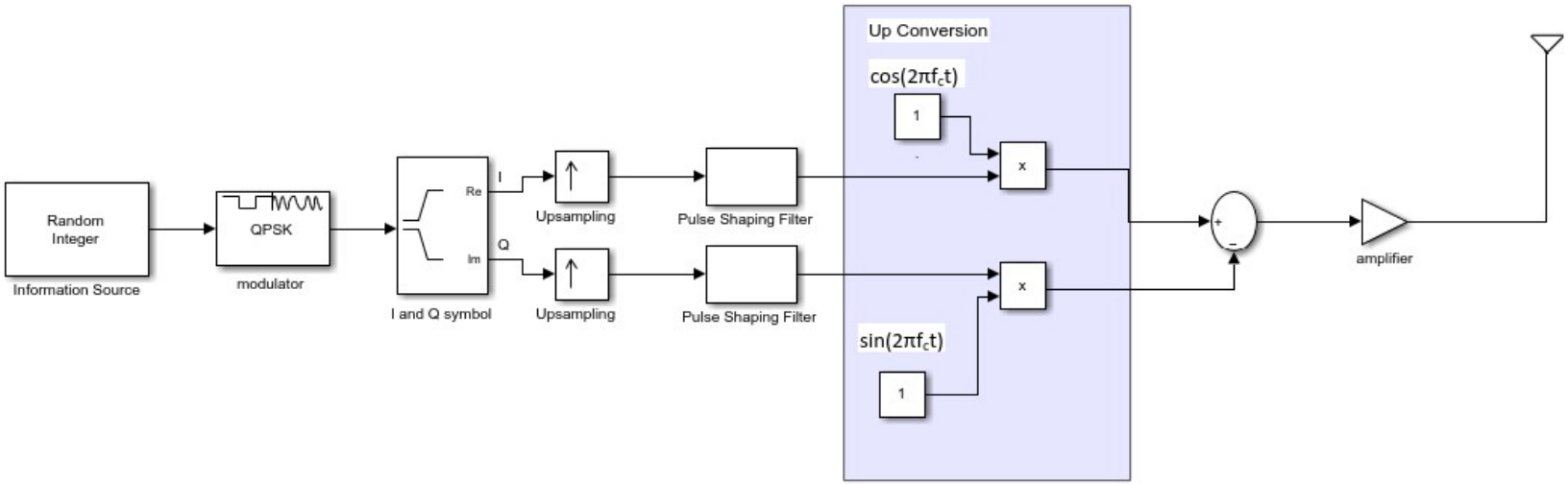

Figure 1. Simplified representation of the transmitter. Adapted from [9].

The transmitter consists of several parts. First, is the information source. For this study, the information source is a stream of symbols where each symbol is a random integer number from 0 to 3. For this experiment, 10^5 symbols were generated. Figure 2 is a display of the first 15 symbols.

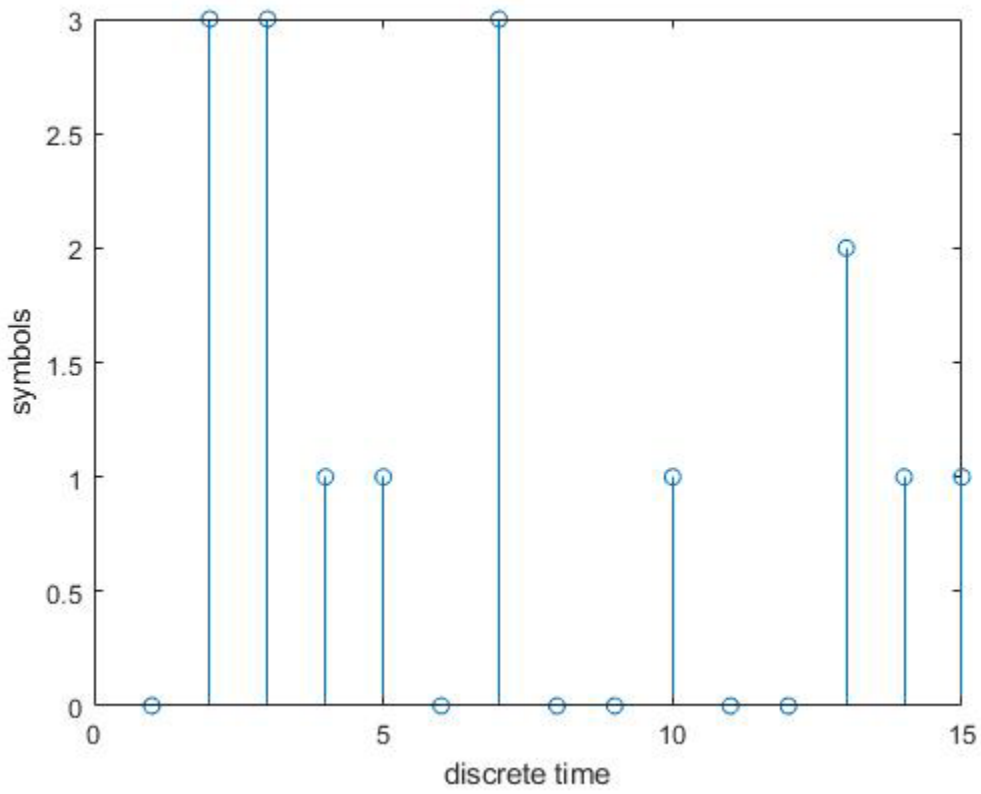

Figure 2. Symbol stream in discrete time

It is necessary that these symbols be digitally processed [9]. The next step after creating these symbols is to transform them into binary information. In Table 1, the correspondence of the generated symbols in binary form, using a Gray code [9], is shown. The Gray code allows only one bit change between adjacent symbols [9], as can been seen in Figure 3. The advantage of using the Gray code is further analyzed in Section II.C.

Table 1. 4-ary symbol coding example

Symbol	Code
0	00
1	01
2	11
3	10

The second block in Figure 1 is the QPSK modulator. The QPSK modulator is responsible for modulating the carrier phase according to the message symbols. Each symbol, or each pair of bits, is mapped to one of the four possible phases:

$$\left(\frac{\pi}{4}, \frac{3\pi}{4}, \frac{5\pi}{4}, \frac{7\pi}{4}\right).$$

The constellation diagram in Figure 3 is a graphical representation of the QPSK modulated symbols. Each symbol is separated from each adjacent symbol by 90° in phase. Thus, each of the four possible phase states are represented. The distance of each state from the origin $O(0,0)$ indicates the symbol energy. In this plot, the horizontal and vertical axes are amplitudes normalized by the factor of $1/\sqrt{E}$, where E is the energy per bit [9].

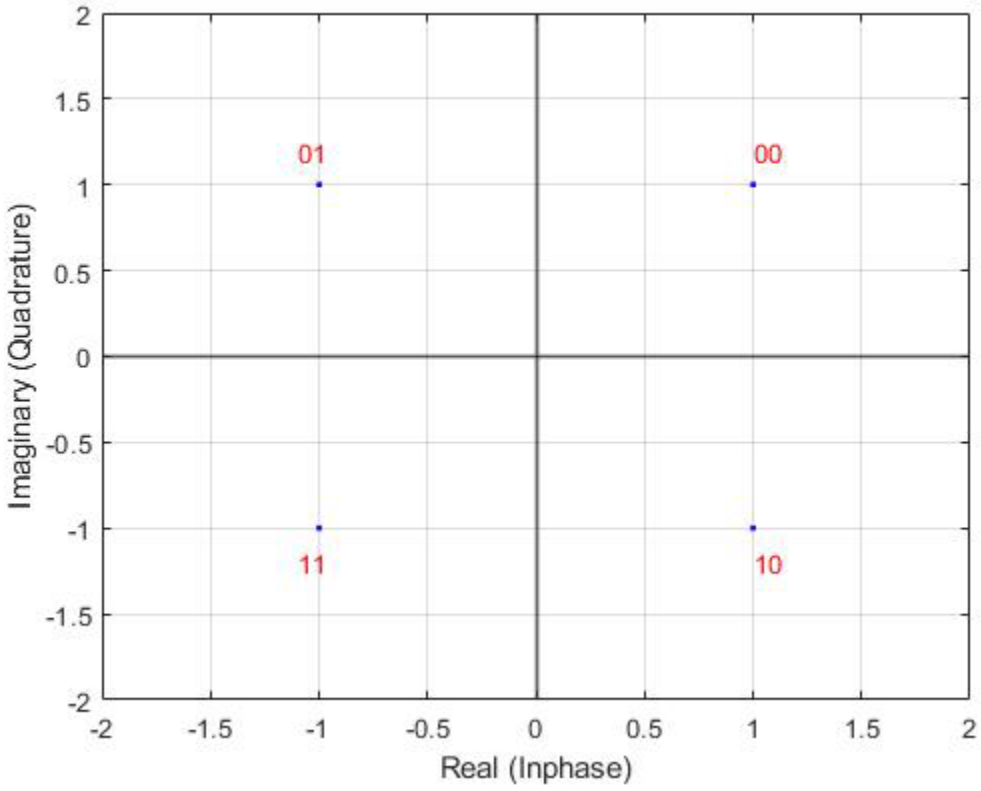

Figure 3. QPSK constellation diagram

Continuing the explanation of the transmitter in Figure 1, the third block splits the QPSK signal into the in phase (I) and quadrature (Q) signals (or I and Q channels). The I and Q signals are displayed on the Cartesian axes in Figure 3 and represent the real and imaginary parts of the complex envelope of the modulated signal [9].

Next is the up-sampling block, which resamples a discrete time signal [10]. The discrete time signal is up-sampled by factor of *N* by appending *(N-1)* zeros between each sample. This idea is illustrated in Figure 4. The purpose of the up-sampling is to increase the sampling rate of the discrete time signal, which is very useful for further processing of the signal, such as pulse shaping [10].

Pulse shaping is a process of modifying the digital signal to ensure that it has the desirable shape to minimize intersymbol interference (ISI). ISI is a phenomenon in digital communications when the transmitted symbols interfere with each other, producing

distortion in the received signal. For zero ISI in communications, Nyquist pulses are used [9]. For this research, a Nyquist pulse of the form of a square root raised cosine (SRRC) was used [9], and it is illustrated in Figure 5.

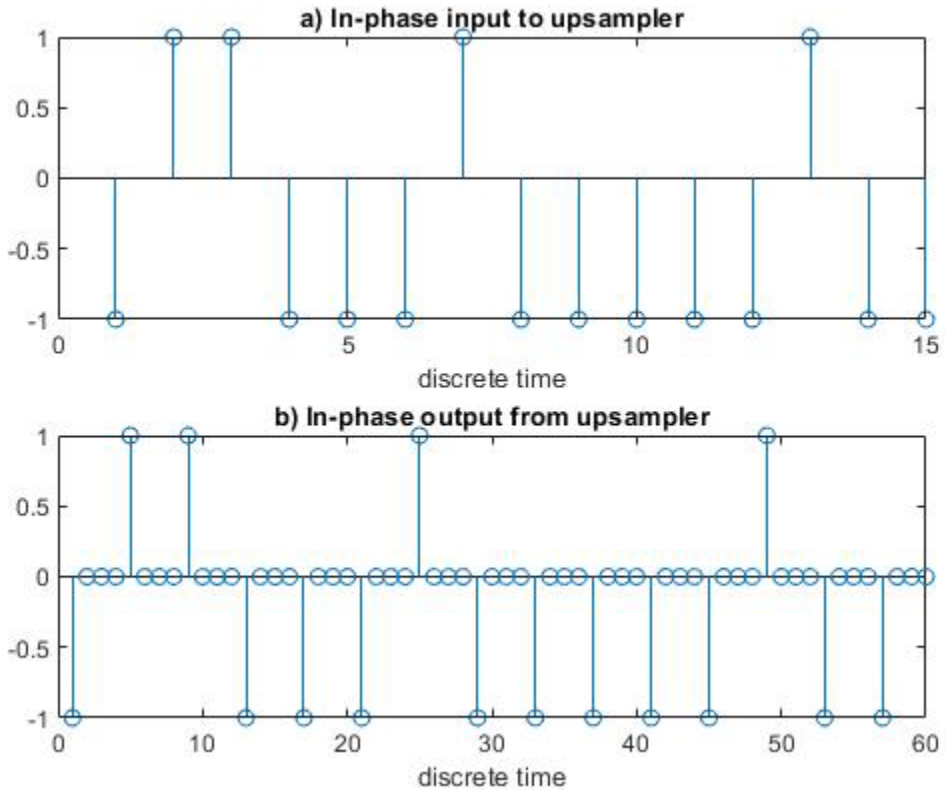

Figure 4. Up-sampling by factor of N=4

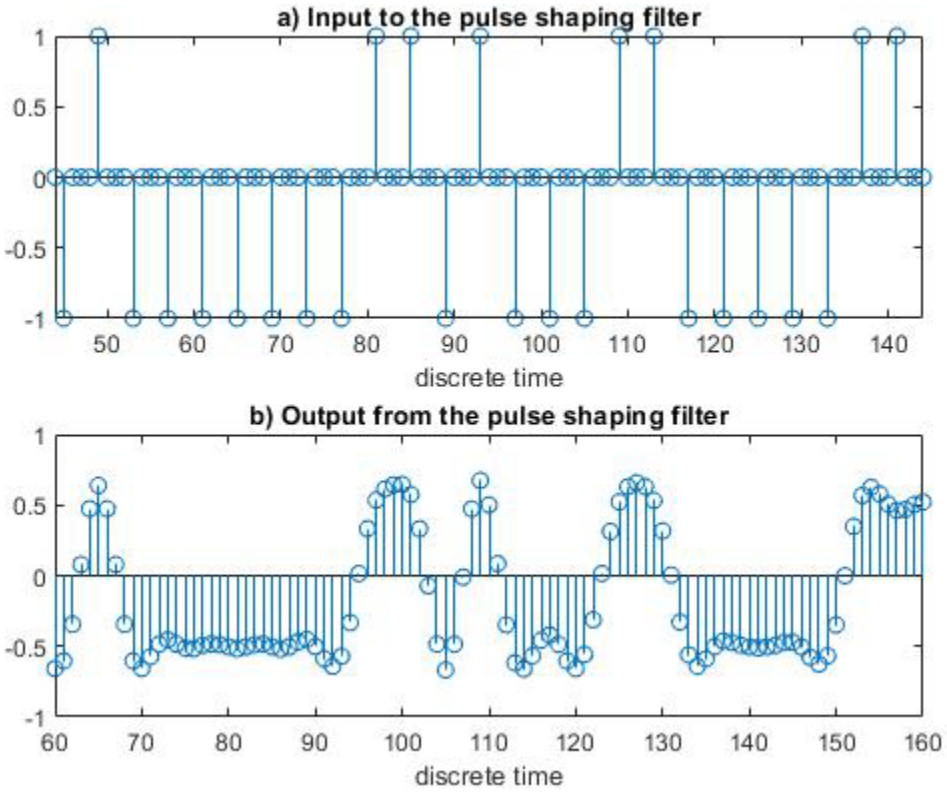

Figure 5. Square root raised cosine pulse shaping

Finally, for the signal to be transmitted, it needs to be upconverted from baseband to the carrier frequency f_c and then amplified before being transmitted through the channel. Upconversion is the process through which the baseband signal (signal with frequencies close to zero) are converted to higher frequencies [9]. The procedure of the upconversion is illustrated in Figure 1. As mentioned in [9], we can analyze the communications system at baseband frequency or at radio frequency.

B. CHANNEL

The channel is the medium through which information is transmitted from the transmitter to the receiver. There are many types of channels such as wired or wireless connections, fiber optic cables, etc. Channels are of crucial importance in communications because they can introduce attenuation, noise, distortion, and other types of interference that can degrade the quality of the transmitted data [9]. In this thesis, it has been assumed

that the channel introduces only additive, white Gaussian noise and no other distortion or interference.

Various techniques are frequently used in digital communication systems to mitigate these effects and ensure reliable transmission. As defined in this thesis, multiple receivers are used to limit the effect of noise on the transmitted signal. The transmitted signal compared to the received signal is shown in Figure 6. In this figure the transmitted signal is depicted in blue, and the received signal is depicted in red. The received signal is the transmitted signal after having been distorted by the introduction of additive, white Gaussian noise.

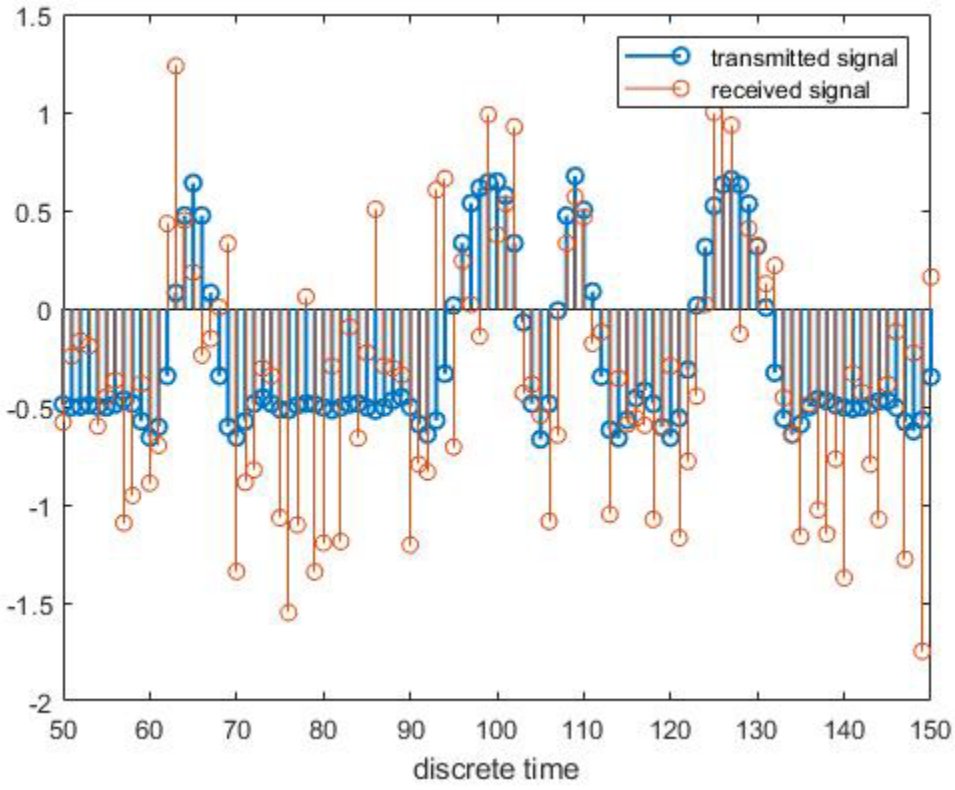

Figure 6. The transmitted and the received signal

C. RECEIVER

The receiver follows the opposite procedure of the transmitter. A simplified representation of the receiver is shown in Figure 7.

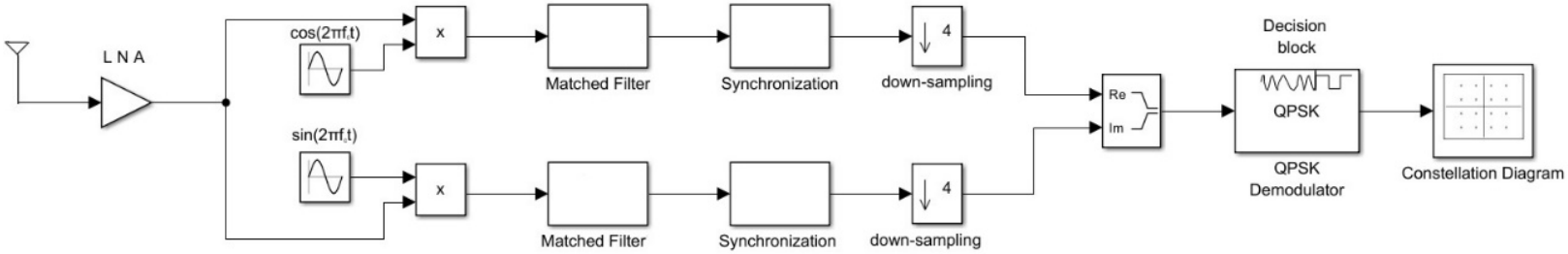

Figure 7. Simplified representation of the receiver. Adapted from [9].

Firstly, the received signal is amplified by a low noise amplifier (LNA). In this thesis it has been assumed that the LNA does not introduce any noise to the received signal. However, there is always thermal noise in every electric circuit which is caused by the motion of the electrons in the components of the circuit such as resistors and wires [9]. The assumption that the LNA does not introduce any noise does not harm the result from the performed research. This is true because all noise produced in the receiver in this experiment is accounted for by an equivalent amount of noise introduced at the receiving antenna.

Afterward, the received signal must be downconverted, as can be seen in Figure 7. The procedure of the downconversion is similar to that of the upconversion. The received signal after being amplified by the LNA is mixed with two local oscillator (LO) signals at the carrier frequency but with a 90° difference in phase [9], [10]. The resulting signals pass through the matched filter (MF). The purpose of the MF is to maximize the SNR at the output of the filter at the sampling time [9], [10]. It is mentioned in [9] and [10] that the impulse response of the MF of the receiver is matched to the impulse response of the pulse shaping filter at the transmitter. If the impulse response of the pulse shaping filter at the transmitter is $s(t)$, then the impulse response of the MF should be $h(t)=s(T-t)$, where T is the symbol period [9], [10].

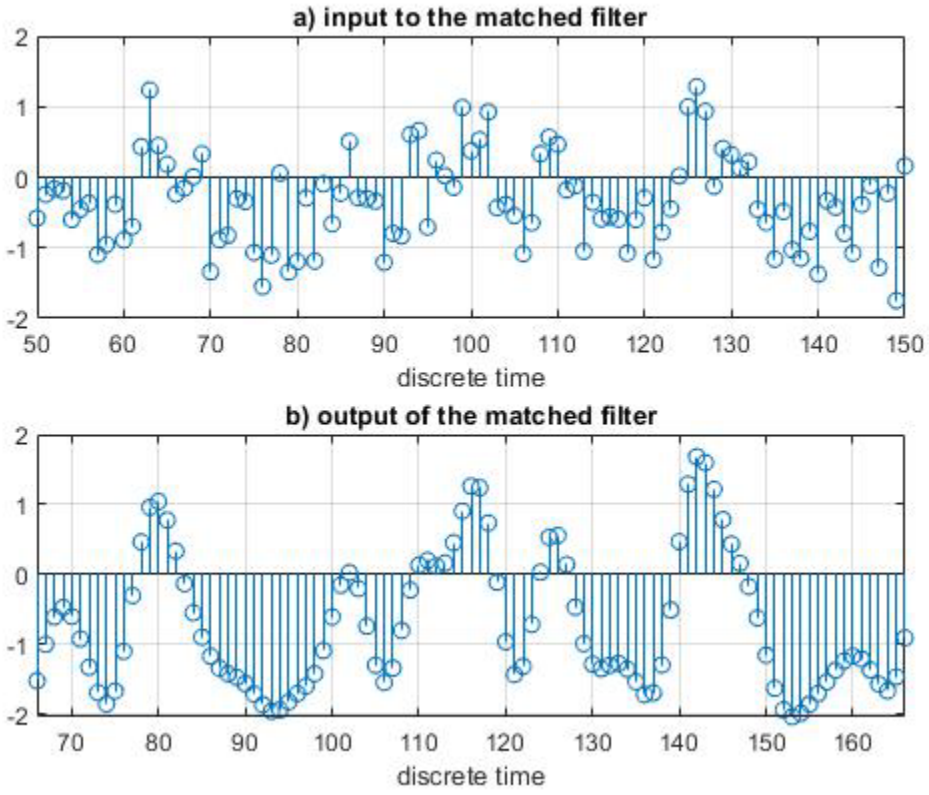

Figure 8. Signal before and after the matched filter

The output of the MF enters the synchronization block, however, in this experiment it is assumed that the transmitter and receiver are perfectly synchronized and no reference is made to synchronization techniques [10].

Both parts of the signal, after being synchronized, are downsampled. Down-sampling is the opposite procedure of up-sampling. It is used to decrease the data rate of the received signal by a factor of *N* by keeping every *N-th* sample of the received signal. In this receiver the down-sampler chooses the signal value at the moment that maximizes the SNR and produces the optimum decision statistic. Decision statistics are the parameters that are used by the decision block in order to determine the received symbol [11]. The received signal after the down-sampling procedure is illustrated in Figure 9.

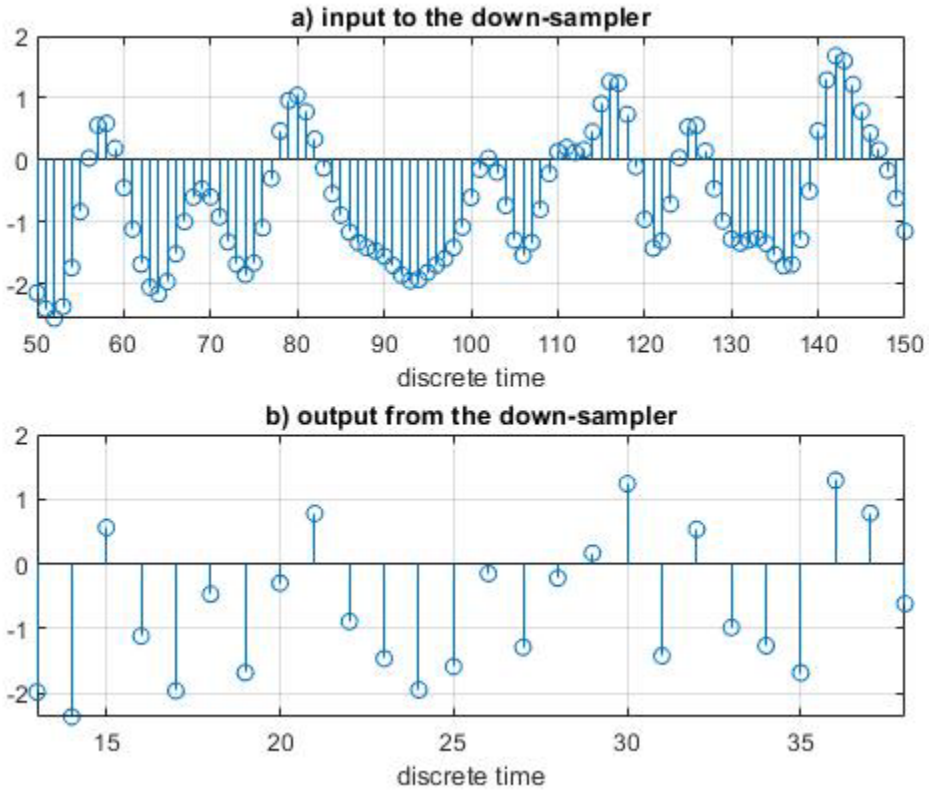

Figure 9. Input and output from the down-sampler

To decode the information in the received signal, the I and Q down-sampled components enter the QPSK demodulation block. In this block the combinations of the I and Q signals, which are also known as the *decision statistics*, are compared with the four possible phase states to determine the received symbol. This decision process is carried out by comparing the reference phases, $\frac{\pi}{4}, \frac{3\pi}{4}, \frac{5\pi}{4}, \frac{7\pi}{4}$, with the phase of the incoming signal. For each symbol, the quadrant for point (I, Q) determines the receiver decision. Any errors due to the introduced noise or due to poor synchronization can lead to incorrect decoding of the transmitted data. The constellation diagram for QPSK demodulation of the 10^5 random integers that were generated for this experiment are illustrated in Figure 10. Each of the four noiseless symbols are represented by a red "x" at the positions $(\pm 1, \pm 1)$. The positions $(\pm 1, \pm 1)$ indicate that the amplitudes of I and Q components are normalized by

the factor $1/\sqrt{E}$, where E is the average energy per bit. The distance from the origin $O(0,0)$ corresponds to the normalized symbol energy [9], [10].

The importance of using the Gray code instead of the traditional binary representation is illustrated in Figure 10. In traditional binary codes, there is more than one bit change between adjacent symbols. If one symbol is incorrectly received in the adjacent quadrant, then in the case of the Gray code there is only one bit error, while in the traditional binary code there may be two bit errors [9].

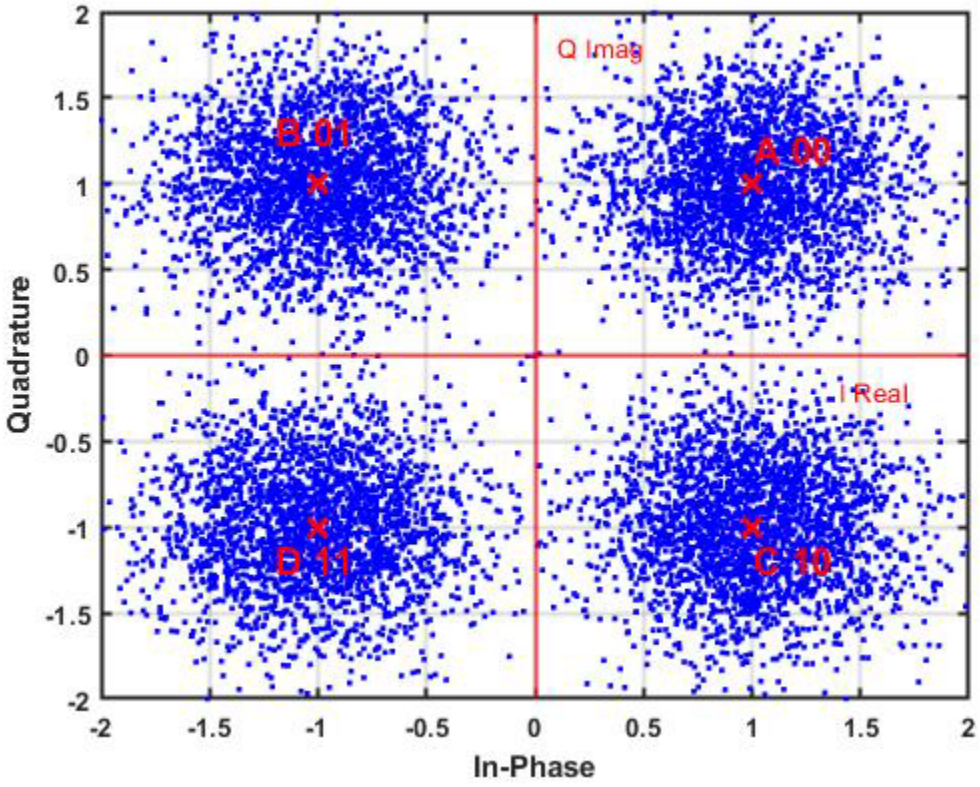

Figure 10. QPSK constellation diagram with Gray code

In this thesis, three new types of receivers are introduced. These three types of receivers process the received signals in a way that is similar to the procedure described above and are analyzed in more detail in Chapter IV.

D. SNR AND E_b/N_0

SNR and E_b/N_0 are two particularly important figures of merit in analog and digital communications that are related to the quality of the received signal. SNR is a crucial parameter in analog communications. It represents the ratio of average signal power to average noise power [9] and is commonly expressed in decibels [dB].

E_b/N_0 is a figure of merit that is used in digital communications and is also expressed in decibels [dB]. E_b is the average energy per bit and can be calculated as the transmitted signal power S divided by the bit rate R_b. N_0 is the one-sided noise power spectral density and can be calculated as the noise power N divided by the noise equivalent bandwidth W of the signal:

$$\frac{E_b}{N_0} = \frac{S/R_b}{N/W} = (SNR)\left(\frac{W}{R_b}\right) \text{ [10].}$$

A plot of the probability of bit error P_B versus E_b/N_0 is one of the most essential performance indicators in digital communication systems. In Figure 11, the probability of bit error for QPSK is illustrated. For a given probability of error, the higher the E_b/N_0 that is required, the less efficient the system. Vice versa, the smaller the E_b/N_0 that is required, the more efficient the system.

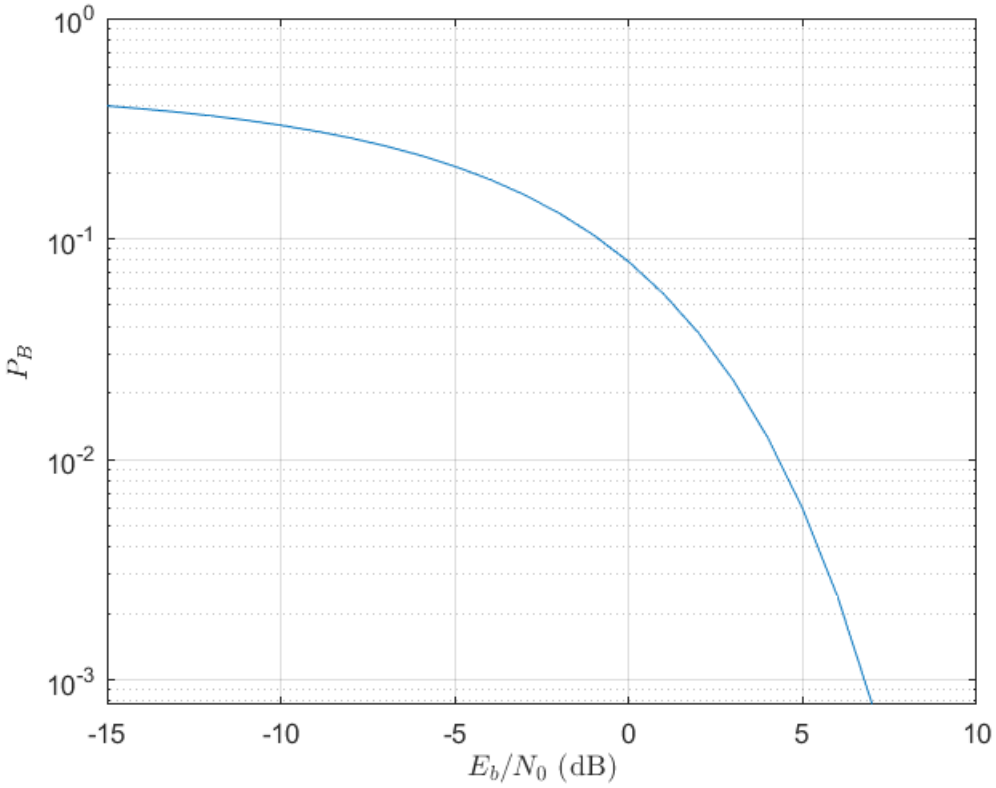

Figure 11. *BER* for QPSK. Adapted from [9].

E. WHITE NOISE

The basic characteristic of white noise is that it has a constant power spectral density across all frequencies [10]. It has the same amount of noise power for all frequencies. The power spectral density (PSD) of additive, white Gaussian noise is shown in Figure 12. The PSD describes how the signal power is distributed across the frequencies [12].

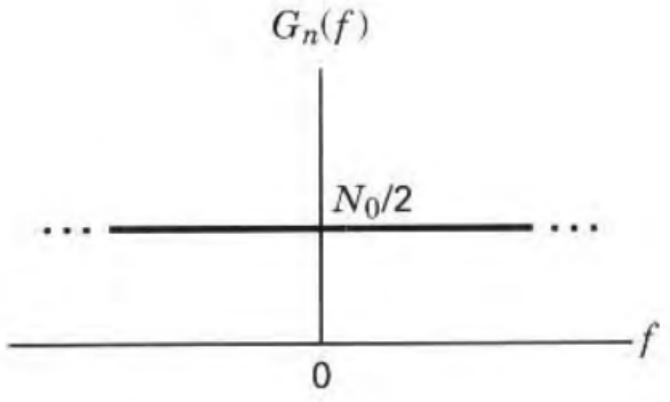

Figure 12. Power spectral density of white noise. Source: [9].

The PSD of white Gaussian noise is $G_n(f) = N_0/2 \ \frac{W}{Hz}$, where the factor of 0.5 is included because it is a two-sided PSD. Finally, the average power P_n of the white Gaussian noise is infinite because the bandwidth is infinite, as shown by:

$$P_n = \int_{-\infty}^{\infty} \frac{N_0}{2} df \rightarrow \infty \text{ [9].}$$

F. BIT ERROR RATE IN QPSK

To better understand the performance of the receivers that were used in this experiment, it is wise to analyze the probability of error in QPSK. In QPSK the probability of bit error is

$$P_B = Q\left(\sqrt{\frac{2E_b}{N_0}}\right) \text{ [9].}$$

In this section, analysis is shown to derive this equation. In QPSK, the transmitted signal is of the form

$$s_i(t) = \begin{cases} \sqrt{\frac{2E}{T}} \cos\left(2\pi f_c t + (2i-1)\frac{\pi}{4}\right), & 0 \le t \le T \\ 0, \ o.w. \end{cases} \tag{2.1}$$

where E is the transmitted energy per symbol, T is the symbol period, f_c is the carrier frequency, and $i \in \{1, 2, 3, 4\}$ [9].

In digital communications, the symbols in (2.1) are often represented by symbol vectors. These vectors define the signal space. The Gram-Schmidt approach can be used to generate an orthogonal collection of basis functions that can be used to describe the digital signal space [11]. Based on the Gram-Schmidt procedure as analyzed in [11], the QPSK orthonormal basis functions can be expressed by the two functions

$$\phi_1(t) = \sqrt{\frac{2}{T}} \cos\left(2\pi f_c t\right) I_{[0,T]}(t)$$

and

$$\phi_2(t) = \sqrt{\frac{2}{T}} \sin\left(2\pi f_c t\right) I_{[0,T]}(t) .$$

where the I is the indictor function and

$$I_{[0,T]}(t) = \begin{cases} 1, & 0 \le t \le T \\ 0, & \text{otherwise} \end{cases} .$$

Considering the trigonometric identity $\cos(A+B) = \cos A \cos B - \sin A \sin B$ and the orthonormal basis functions, the transmitted signal can be further expanded as

$$s_i(t) = \sqrt{E}\cos\left((2i-1)\frac{\pi}{4}\right)\varphi_1(t) - \sqrt{E}\sin\left((2i-1)\frac{\pi}{4}\right)\varphi_2(t) .$$

Therefore, the signal vectors are given as

$$\mathbf{s}_i = \begin{bmatrix} s_{i_1} \\ s_{i_2} \end{bmatrix} = \begin{bmatrix} \sqrt{E}\cos\left((2i-1)\frac{\pi}{4}\right) \\ \sqrt{E}\sin\left((2i-1)\frac{\pi}{4}\right) \end{bmatrix},$$

which can be expressed as

$$s_1 = \begin{bmatrix} \sqrt{E/2} \\ \sqrt{E/2} \end{bmatrix}, \; s_2 = \begin{bmatrix} -\sqrt{E/2} \\ \sqrt{E/2} \end{bmatrix}, \; s_3 = \begin{bmatrix} -\sqrt{E/2} \\ -\sqrt{E/2} \end{bmatrix}, \text{ and } s_4 = \begin{bmatrix} \sqrt{E/2} \\ -\sqrt{E/2} \end{bmatrix}.$$

The representation of these symbol vectors creates the QPSK constellation diagram that was initially reported in Section II.A, and its normalized form is illustrated in Figure 13.

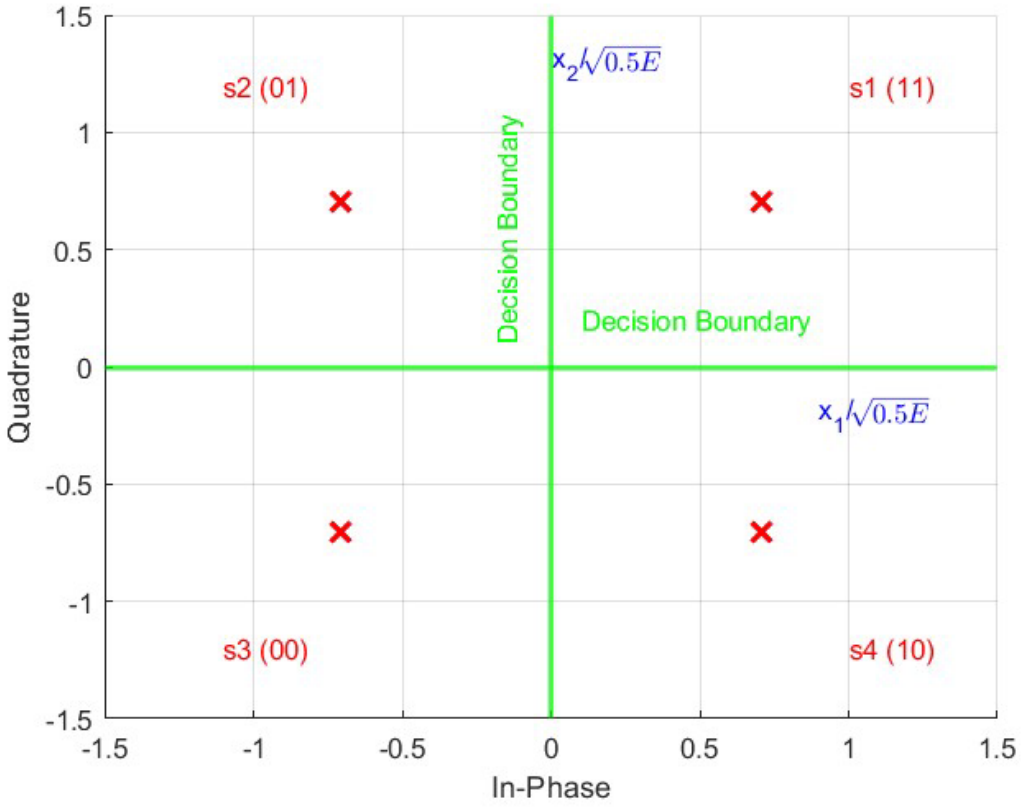

Figure 13. QPSK constellation diagram with Gray code. Adapted from [9].

As mentioned earlier in this section, the received signal is assumed to be distorted only by white Gaussian noise. So, the received signal is $x(t) = s_i(t) + w(t)$, where $w(t)$ is the white Gaussian noise. The characteristics of white Gaussian noise are discussed in Section II.E. For each received symbol, $x(t)$, the receiver calculates two decision statistics,

x_1 and x_2. The vector (x_1, x_2) can be viewed in the constellation diagram in Figure 13 and the decision statistics are

$$x_1 = \pm\sqrt{\frac{E}{2}} + w_1 \quad \text{and} \quad x_2 = \pm\sqrt{\frac{E}{2}} + w_2,$$

where w_1 and w_2 independent zero mean Gaussian random variables. Since white Gaussian noise has zero mean,

$$E[x_1] = E[x_2] = \pm\sqrt{\frac{E}{2}}$$

and

$$var(x_1) = var(x_2) = \frac{N_0}{2}$$

as shown in [9], [12].

If the symbol $s_1(t)$ as depicted in Figure 13 is transmitted, that indicates that

$$E[x_1] = E[x_2] = \sqrt{\frac{E}{2}}.$$

The probability of the correct symbol decision given that the $s_1(t)$ is transmitted is

$$P_{c|s_1} = \Pr(x_1 > 0 \cap x_2 > 0 | \boldsymbol{s}_1).$$

As indicated in [12], when the two random variables A and B are independent, this yields $P(A \cap B) = P(A)\,P(B)$, which indicates that

$$P_{c|s_1} = \Pr(x_1 > 0 | s_1)\,\Pr(x_2 > 0 | s_1),$$

because the decision statistics are independent of each other. Further expansion indicates that

$$P_{c|s_1} = \int_0^\infty f_{x_1}(x_1 | s_1)\,dx_1 \int_0^\infty f_{x_2}(x_2 | s_1)\,dx_2,$$

where

$$f_{x_1}(x) = f_{x_2}(x) = f_x(x) = \frac{1}{\sqrt{2\pi\sigma^2}} e^{\left(-\frac{(x-\mu)^2}{2\sigma^2}\right)},$$

μ is the mean, and σ^2 is the variance. It is known from [12] that

$$\Pr\left(x_1 > 0 | s_1\right) = 1 - Q\left(\sqrt{\frac{E}{N_0}}\right).$$

This implies

$$P_{c|s_1} = \left[1 - Q\left(\sqrt{E/N_0}\right)\right]^2,$$

where the Q-function is defined in [12] and is

$$Q(x) = \frac{1}{\sqrt{2\pi}} \int_x^\infty \exp\left(-\frac{t^2}{2}\right) dt.$$

Due to symmetry, probability of symbol error is the same regardless of which symbol is sent, i.e.,

$$P_{e|s_1} = P_{e|s_2} = P_{e|s_3} = P_{e|s_4} = 1 - P_c. \tag{2.2}$$

Therefore,

$$P_e = 2Q\left(\sqrt{\frac{E}{N_0}}\right) - \left[Q\left(\sqrt{\frac{E}{N_0}}\right)\right]^2 \approx 2Q\left(\sqrt{\frac{E}{N_0}}\right), \tag{2.3}$$

which is the probability of symbol error in QPSK. In QPSK, two bits are used for every symbol. So, $E = 2E_b$ where E_b is the received energy per bit. Finally, the symbol error rate is

$$P_e = 2Q\left(\sqrt{\frac{2E_b}{N_0}}\right). \tag{2.4}$$

As shown in [9], when the Gray code is used,

$$P_B \approx \frac{P_e}{\log_2 M}$$

(for $P_e \ll 1$) where $M = 4$ for QPSK. Therefore, the bit error rate in QPSK is

$$P_B = Q\left(\sqrt{\frac{2E_b}{N_0}}\right). \tag{2.5}$$

The *BER* versus E_b / N_0 for QPSK is shown in Figure 11.

G. CONCLUSION

In conclusion, the analysis of communications theory is especially important for the successful design of a communication system that leverages multiple receivers. In Section A, the components of the transmitter were analyzed. Moreover, the QPSK modulation technique is highlighted. In Section B, we emphasized the impact of the channel on the transmitted signal. Information about the components of the receiver were given in Section C. Moreover, emphasis is given to the QPSK demodulation procedure. The significance of the E_b / N_0 and white Gaussian noise are explored in sections D and E, respectively. Finally, the probability of error in QPSK modulation was analyzed in Section F. In general, this background knowledge chapter offers the information needed to understand the design of the multiple-receiver communications systems that is presented in Chapter III.

III. RADIO DESIGN

In this chapter, the analysis of the design of the three types of receivers that were used in this research are presented. For the purpose of this document, these receivers are named as super-receivers type-A, -B and -C, respectively. These names were chosen in order to distinguish them from the ordinary QPSK receiver that was described in Chapter II. These super-receivers include multiple modified copies of the QPSK receiver that was illustrated in Figure 7. The goal of this research is to combine the received signals from the multiple branches to improve receiver performance.

A. SUPER-RECEIVER TYPE-A

In the case of super-receiver type-A, K individual signals are combined before amplification by the LNA. Super-receiver type-A is illustrated in Figure 14.

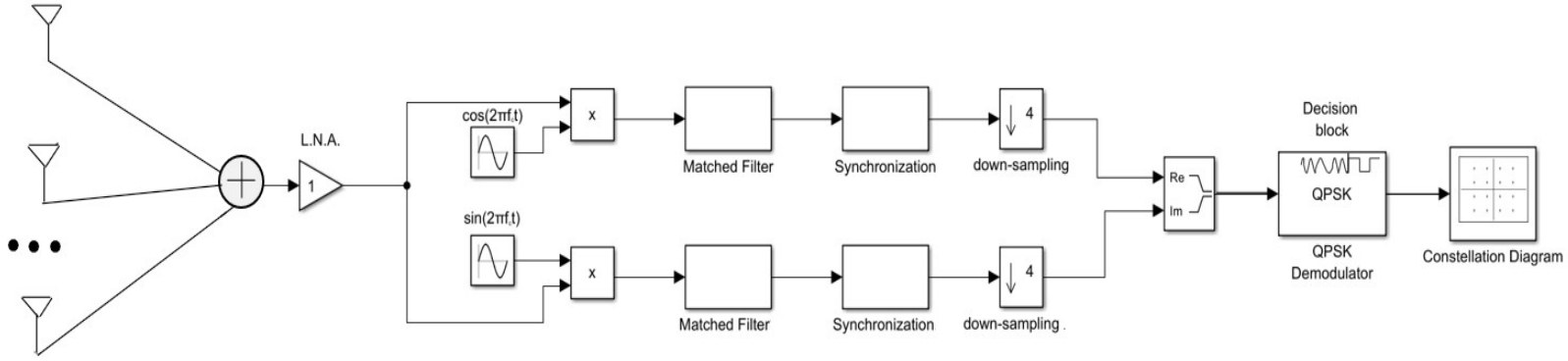

Figure 14. Super-receiver type-A

In the context of the conducted research, several antennas receive the transmitted signal. The antennas are transducers that convert the received electromagnetic field into an electric signal [9]. The total received power from every antenna should be equal to the sum of the received power from each antenna. The received power from one antenna is given by

$$P_r = \frac{P_t G_t A_{er}}{4\pi d^2},$$

where P_t is the transmitted power, G_t is the gain of the transmitting antenna, A_{er} is the effective area of the receiving antenna and d is the distance between transmitter and receiver [9]. The physical area of the antenna, A_p, and effective area, A_e, are related by the efficiency parameter η, $A_e = \eta A_p$ [9]. This relationship indicates that the total received power from K receivers is

$$P_{r_{type\ A}} = \frac{P_t G_t \eta K A_p}{4\pi d^2}.$$

Therefore, the received power from super-receiver type-A, which has K antennas each of physical area A_p, is K times the received power from one receiver with the same antenna.

The received noise power is $N = \kappa T^\circ W$, where κ is the Boltzmann's constant, T° is the system noise temperature, and W is the bandwidth [9]. The single-sided noise power spectral density N_0 is $N_0 = \frac{N}{W} = \kappa T^\circ$, which indicates that N_0 depends only on system noise temperature. For this research, the assumption was made that the system noise temperature for all types of super-receivers is the same as that of the ordinary QPSK receiver.

Finally, the total received energy per bit for super-receiver type-A is proportional to the total area of the antennas in super-receiver type-A. Thus,

$$E_{b_{type\ A}} = K \cdot E_{b_{one\ receiver}}$$

and, consequently,

$$\left(\frac{E_b}{N_0}\right)_{type\ A} = K\frac{E_b}{N_0}.$$

This result is extremely useful in calculating the theoretical probability of error in this type of receiver. Taking into account the $\left(E_b/N_0\right)_{type\ A}$ and the analysis in Section II.F, the theoretical value of the *BER* is

$$P_B = Q\left(\sqrt{K\frac{2E_b}{N_0}}\right). \tag{3.1}$$

B. SUPER-RECEIVER TYPE-B

In this second technique, the super-receiver type-B combines the K individual complex Gaussian random variables to form the final decision statistics. The super-receiver type-B is illustrated in Figure 15.

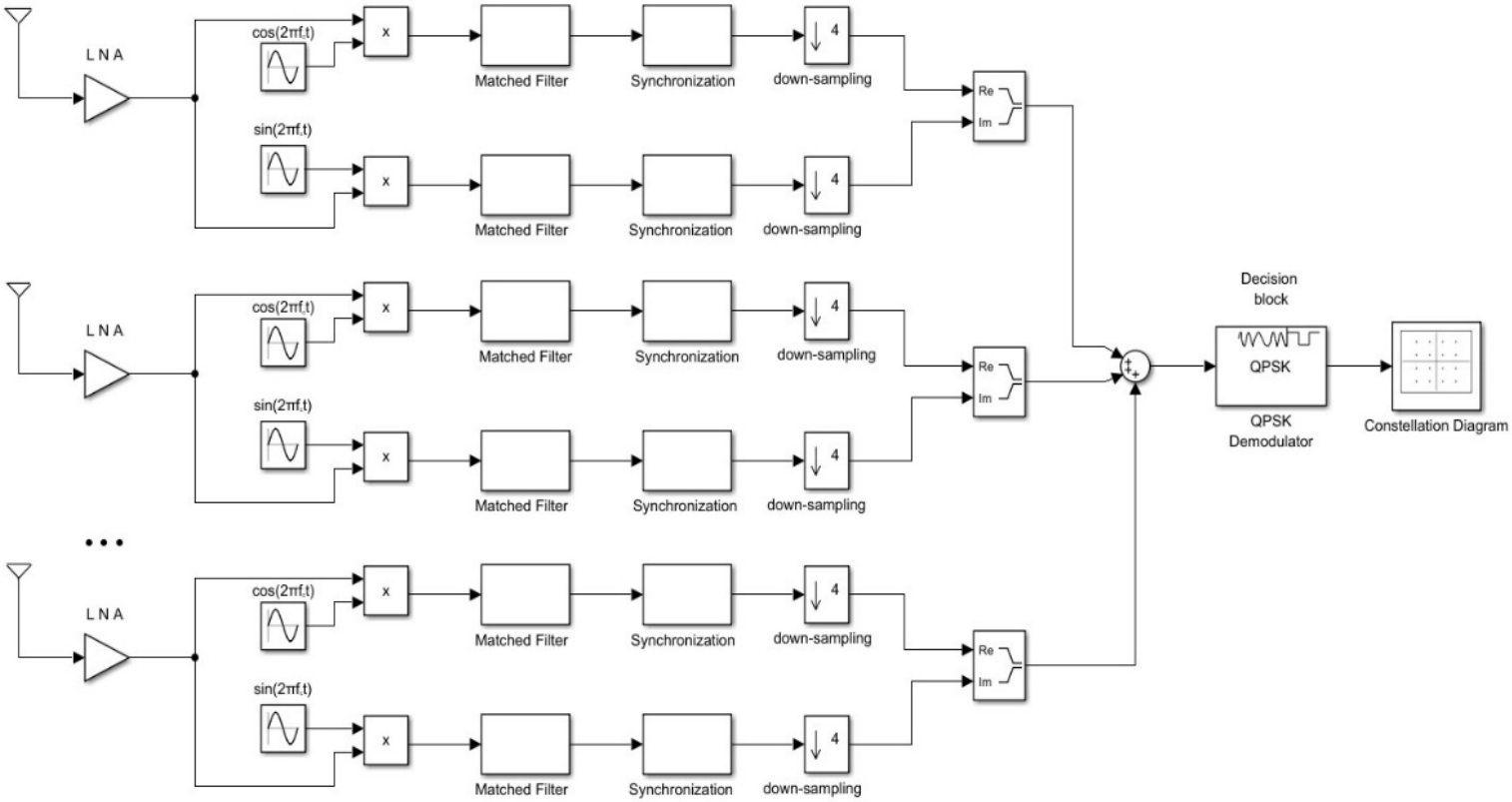

Figure 15. Super-receiver type-B

In the case of super-receiver type-B, the complex random variables are added together to form the decision statistics. It should be considered that all the procedures that take place between the antenna and QPSK demodulator are linear, and the total introduced noise is assumed to be the same as has been counted for super-receiver type-A. Consequently, the decision statistic and therefore the demodulation results are expected to be the same as in the case of super-receiver type-A. The total received power for this case and the $\left(E_b/N_0\right)_{type\ B}$ are equal to what was found for super-receiver type-A,

$$\left(\frac{E_b}{N_0}\right)_{type\ B}=\frac{KE_b}{N_0}.$$

This result shows that the theoretical *BER* for this case of receiver is

$$P_B=Q\left(\sqrt{K\frac{2E_b}{N_0}}\right).$$

If each branch of the receiver introduces the same noise power as one receiver, then the system is expected not to show any improvement to the *BER*, because then the

$$\left(\frac{E_b}{N_0}\right)_{type\ B}=\frac{KE_b}{KN_0}=\frac{E_b}{N_0}.$$

In other words, the performance of the systems is influenced by noise introduced from each branch of the receiver.

C. SUPER-RECEIVER TYPE-C

This is the last type of receiver that was used in the conducted experiment. The super-receiver type-C combines the *K* individual symbol decisions to form a single composite symbol decision. The super-receiver type-C is illustrated in Figure 16.

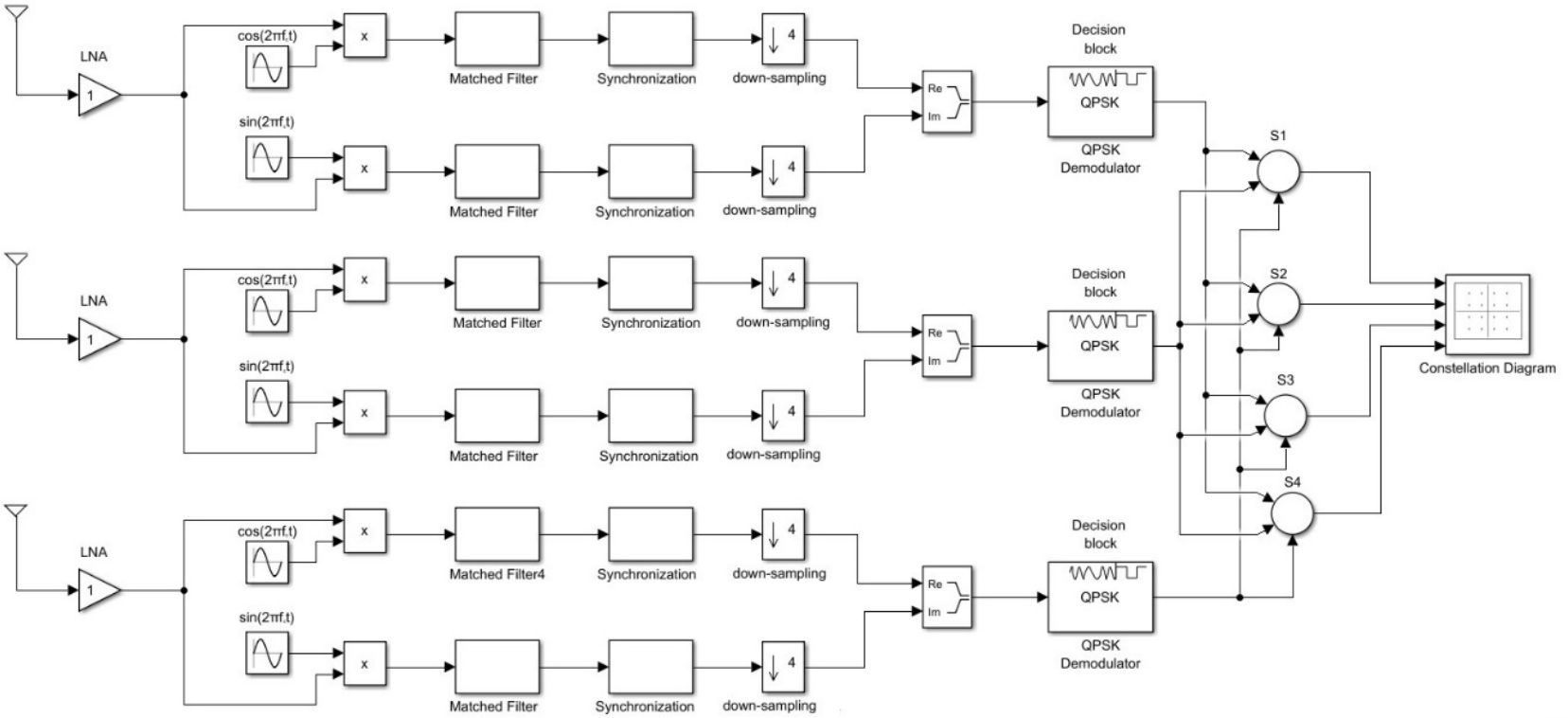

Figure 16. Super-receiver type-C

This receiver counts how many branches decide in favor of each symbol s_1, s_2, s_3 and s_4, and then selects the symbol with the largest tally. In super-receiver type-C, each branch works individually, making its own symbol decision. For a theoretical calculation of the *BER*, a different approach is needed because the way this receiver works is different from the previous two. In this case, every QPSK branch receiver receives each symbol and makes the symbol decision without any improvement to the values of E_b/N_0. The probability of bit error for each branch is

$$P_B = Q\left(\sqrt{\frac{2E_b}{N_0}}\right)$$

as for the one receiver [9].

The symbol decisions from each branch are combined for the final single composite symbol decision to be made. Super-receiver type-C counts how many branch decisions are in favor of each symbol and makes the final decision based on the symbol that is chosen most. For example, if super-receiver type-C has five branches, and if three of the branches choose the symbol s_4 and the rest choose another symbol, then the final decision of the super-receiver type-C would be symbol s_4.

Let N_i denote the number of branches that choose symbol $\boldsymbol{s}_i$. If $\boldsymbol{s}_1$ is transmitted, a symbol decision error will result if

$$N_1 < N_2 \text{ or } N_1 < N_3 \text{ or } N_1 < N_4.$$

Therefore, the conditional symbol error probability is

$$P_{e|s_1} = \Pr\left(N_1 < N_2 \cup N_1 < N_3 \cup N_1 < N_4 | s_1 \text{ is sent}\right). \tag{3.2}$$

An exact calculation of the P_e is challenging, particularly when multiple branches are utilized from the super-receiver type-C. Therefore, an approximation of $P_{e|s_1}$ could be obtained by the union bound, which states that

$$\Pr\left(\bigcup_{i=1}^{M} A_i\right) \le \sum_{i=1}^{M} \Pr(A_i).$$

The union bound is described in [11] and is used to give an upper bound of a probability. By using the union bound, (3.2) leads to

$$P_{e|s_1} \le \Pr(N_1 < N_2 | s_1) + \Pr(N_1 < N_3 | s_1) + \Pr(N_1 < N_4 | s_1). \tag{3.3}$$

Based on the QPSK constellation diagram in Figure 13 back in Chapter 2, the symbol s_1 is adjacent to the symbols s_2 and s_4. Moreover, the assumptions can be made that

$$\Pr(N_1 < N_2 | s_1) = \Pr(N_1 < N_4 | s_1)$$

due to symmetry and

$$\Pr(N_1 < N_3 | s_1) \ll \Pr(N_1 < N_4 | s_1)$$

due to the greater distance between symbols s_1 and s_3. Taking these into account, we can write (3.3) as

$$P_{e|s_1} \approx 2\Pr(N_1 < N_4 | s_1). \tag{3.4}$$

The super-receiver type-C will always give the wrong result when the symbol s_1 is sent if more than the half of the branches receive the symbol s_4. If $N_4 > \frac{K}{2}$, then $N_1 < N_4$ because $\sum_{i=1}^{4} N_i = K$; therefore,

$$\Pr(N_1 < N_4 | s_1) \approx \Pr\left(N_4 > \frac{K}{2} | s_1\right)$$

seems to be a reasonable assumption, and (3.4) leads to

$$P_{e|s_1} \approx 2\Pr\left(N_4 > \frac{K}{2} | s_1\right).$$

Using the binomial distribution, as described in [12] and $\Pr\left(N_4 > \frac{K}{2} | s_1\right)$, we get

$$P_{e|s_1} \approx 2 \sum_{i=K/2+1}^{K} \binom{K}{i} p_{s_4|s_1}^{i} \left(1 - p_{s_4|s_1}\right)^{K-i}.$$

Based on Figure 13 the $p_{s_4|s_1}$ is defined as

$$p_{s_4|s_1} = \Pr\left(x_1 > 0, x_2 < 0 | s_1\right) = \Pr\left(x_1 > 0\right) \Pr\left(x_2 < 0\right)$$

$$= Pr\left(\frac{x_1 - \sqrt{E/2}}{\sqrt{N_0/2}} > -\frac{\sqrt{E/2}}{\sqrt{N_0/2}}\right) Pr\left(\frac{x_2 - \sqrt{E/2}}{\sqrt{N_0/2}} < -\frac{\sqrt{E/2}}{\sqrt{N_0/2}}\right)$$

$$= \left(1 - Q\left(\sqrt{\frac{E}{N_0}}\right)\right) Q\left(\sqrt{\frac{E}{N_0}}\right) \approx Q\left(\sqrt{\frac{E}{N_0}}\right) = Q\left(\sqrt{\frac{2E_b}{N_0}}\right).$$

Finally, the approximation of the symbol error in super-receiver type-C can be calculated from

$$P_{e|s_1} \approx 2 \sum_{i=K/2+1}^{K} \binom{K}{i} \left(Q\left(\sqrt{\frac{2E_b}{N_0}}\right)\right)^{i} \left(1 - Q\left(\sqrt{\frac{2E_b}{N_0}}\right)\right)^{K-i}. \tag{3.5}$$

As already mentioned in Section II.F, and as analyzed in [9],

$$P_B \approx \frac{P_e}{\log_2 M}$$

(for $P_e \ll 1$), and the probability of bit error is

$$P_{B|s_1} \approx \sum_{i=K/2+1}^{K} \binom{K}{i} \left(Q\left(\sqrt{\frac{2E_b}{N_0}}\right)\right)^{i} \left(1 - Q\left(\sqrt{\frac{2E_b}{N_0}}\right)\right)^{K-i}.$$

Finally, due to symmetry, the probability of bit error for super-receiver type-C is

$$P_B \approx \sum_{i=K/2+1}^{K} \binom{K}{i} \left(Q\left(\sqrt{\frac{2E_b}{N_0}}\right)\right)^{i} \left(1 - Q\left(\sqrt{\frac{2E_b}{N_0}}\right)\right)^{K-i}. \tag{3.7}$$

The curves of the theoretical *BER* and the simulated *BER* that were created for this research for super-receiver type-C are illustrated and further analyzed in Section IV.C.

D. CONCLUSION

In this chapter, the radio design for each type of receiver is illustrated, and the theoretical value of bit error rate for each case was determined. It is shown that under the stated assumptions regarding noise sources and antenna sizes, the super-receivers type-A and type-B have the same bit error rate performance. Super-receiver type-C has a different *BER* performance, which is shown in the next chapters to be worse than that of the -A and -B under the assumptions regarding noise and antennas. This explanation is helpful in understanding the radio analysis and the *BER* plots that follow in Chapter IV.

THIS PAGE INTENTIONALLY LEFT BLANK

IV. TESTING

The results from the experiments conducted, along with a thorough analysis of the MATLAB-generated plots, are presented in this chapter. To evaluate the performance of super-receivers type-A and -B, a total of 10^5 random symbols were generated, utilizing 15 QPSK branches. For super-receiver type-C, the experiment involved generating 10^6 random symbols, again by leveraging 15 branches. By increasing ten times more random symbols for the third type of receiver, we aim to gain a clearer understanding of the approximation on the calculation of the *BER* that is explained in Section III.C.

A. BIT ERROR RATE IN SUPER-RECEIVER TYPE-A

The first mention of the super-receiver type-A is made in Section III.A, and its arrangement is shown in Figure 14, in Chapter III. It was shown in Section III.A. that the *BER* for super-receiver type-A is given by equation (3.1),

$$P_B = Q\left(\sqrt{K\frac{2E_b}{N_0}}\right),$$

where K is the number of receivers. Three curves are illustrated in Figure 17. The first one is the simulated *BER* for super-receiver type-A. The second one is the theoretical *BER* for super-receiver type-A, as given in (3.1), and the third one is the theoretical *BER* for one receiver as given in (2.5).

For the simulation of this experiment, MATLAB scripts and functions were utilized. Initially, 10^5 random symbols were generated. These symbols were assigned values $0, 1, 2,$ or 3 with equal probability, $P_{s_i} = 1/4$. Subsequently, these symbols underwent QPSK modulation [9]. Each symbol was represented by a pair of bits as indicated in Table 1. These pairs of bits were then mapped in one of the four quadrants, defining the QPSK phase shift [9] as shown in Figure 3 in Chapter II. This process results in the generation of the I and Q signals. Next, each signal was up-sampled by a factor of four and then passed through the SRRC pulse shaping filters for pulse shaping. The output

of the pulse shaping filters, $s_I[n]$ and $s_Q[n]$, are the signals that were transmitted. In the context of the simulation, it was not necessary to upconvert and amplify the transmitted signal.

These signals, $s_I[n]$ and $s_Q[n]$, form the transmitted complex discrete time signal $s[n]=s_I[n]+js_Q[n]$. The receiver receives the $s_I[n]$ and $s_Q[n]$ after being distorted by noise. The received signal is

$$r[n]=s[n]+w[n]$$

where $w[n]$ is a complex discrete time signal, and represents the additive Gaussian noise,

$$w[n]=w_I[n]+jw_Q[n].$$

Finally, the $r_I[n]$ and $r_Q[n]$ parts of the received signals can be expressed as

$$r_I[n] = s_I[n] + w_I[n] \text{ and}$$
$$r_Q[n] = s_Q[n] + w_Q[n].$$

The $w_I[n]$ and $w_Q[n]$ are independent and take on random values that follow the Gaussian distribution with mean $\mu=0$ and a variance $\sigma^2=\frac{N_0}{2}$. $\frac{N_0}{2}$ is the noise power spectral density as described in Section II.E. In this experiment, diverse values were assigned to the variance of noise, $\frac{N_0}{2}$, with the purpose of generating the *BER* curves. As discussed in Section II.D, E_b/N_0 serves as a crucial metric in evaluating digital communications. Hence, E_b/N_0 values varied from -19 to 9 dB and the probability of bit error was calculated and plotted.

In the case of the super-receiver type-A, the signals received from each of the K branches are added, and the combined signal passes through the MF. Consequently, the combined signal is down-sampled to generate the composite decision statistics. Finally, these composite decision statistics are the input to the QPSK demodulator for the final symbol decisions. The *BER* performance of this entire process in illustrated in Figure 17.

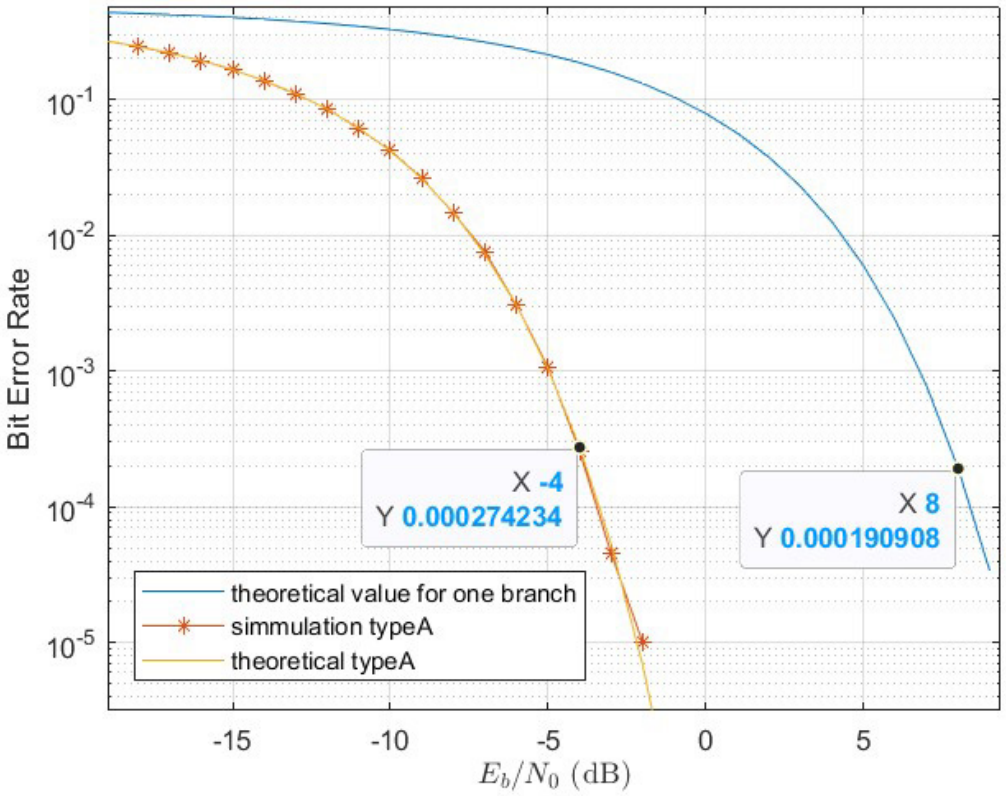

Figure 17. *BER* versus E_b/N_0 for super-receiver type-A

Since the numerical and the analytical results for super-receiver type-A correspond so closely, it seems that they are likely correct. The curves were created by using 15 branches and, therefore, the E_b/N_0 is improved by a factor of 15. That indicates an improvement to the total performance of $10\log_{10}15 \approx 12$ dB, which is illustrated in Figure 17. Finally, since 10^5 random symbols were generated, the theory and simulation correspond closely for $BER > 10^{-4}$.

B. BIT ERROR RATE IN SUPER-RECEIVER TYPE-B

The first mention of the super-receiver type-B is made in Section III.B, and its arrangement is shown in Figure 15 in Chapter III. As it is explained in Section III.B, its *BER* performance is expected to be the same for super-receiver type-A. The *BER* for super-receiver type-B is derived from equation (3.1). The *BER* for super-receivers type-A and

type-B as determined by simulation, the theoretical *BER* for super-receiver type-B, and the theoretical *BER* for one receiver are shown in Figure 18.

The simulation was done exactly as before, the difference being the random variables from each branch are added together after being down-sampled in order to form the decision statistics. Finally, these composite decision statistics enter the QPSK demodulator for the final symbol decision. The resulting *BER* performance is depicted in Figure 18.

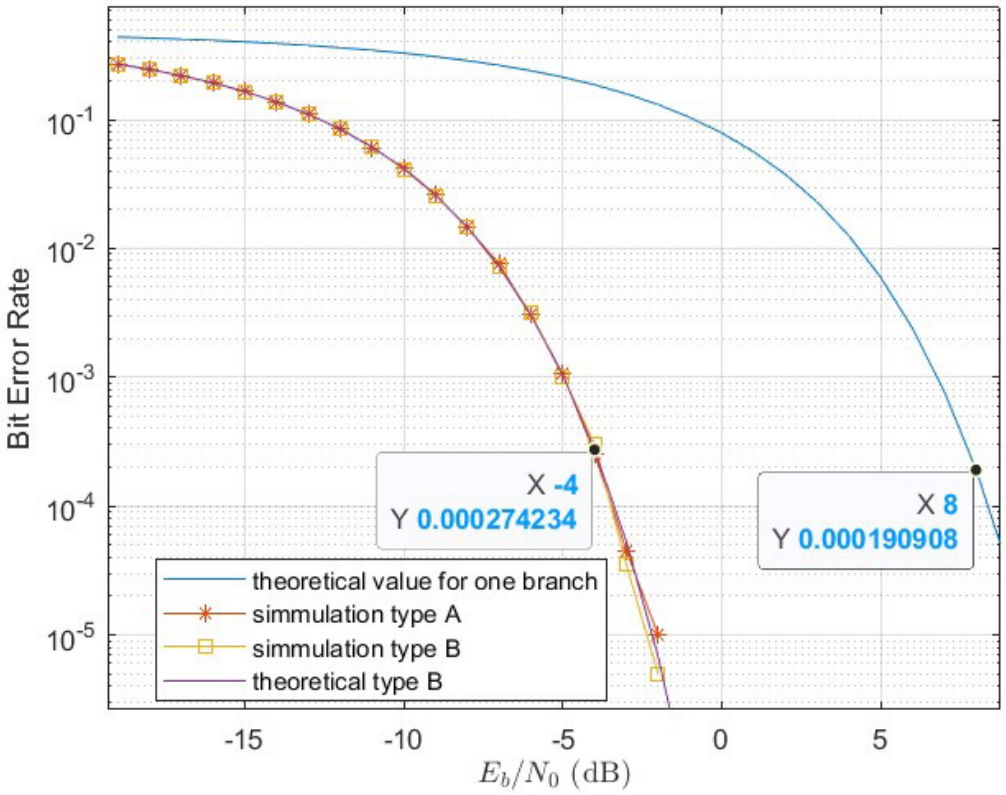

Figure 18. *BER* versus E_b/N_0 for super-receiver type-B

Again, the improvement to the performance is equal to that of super-receiver type-A and it is approximately $10\log_{10}K$. As previously, it is expected that theory and simulation results correspond for $BER > 10^{-4}$. Moreover, as can be seen in Figure 18, the simulated results for super-receiver type-A and type-B are almost equal.

C. BIT ERROR RATE IN SUPER-RECEIVER TYPE-C

The first mention of the super-receiver type-C and the way it works is made in Section III.C. Its arrangement is shown in Figure 16 back in Chapter III. Moreover, in Section III.C, an approximation of the *BER* is calculated. In this section, the *BER* as determined by simulation and by analysis are illustrated.

Again, the simulation was done as described in Section IV.A, with the difference that 10^6 random symbols were generated. For this receiver, the symbol decisions from each branch are tallied and compared to make the final symbol decision. For this experiment a script was created that counts how many branches decide in favor of each symbol, and finally selects the symbol with the largest tally. The resulting *BER* performance is depicted in Figure 19, where the *BER* curves as determined by simulation and analysis for super-receiver type-C with 15 branches and the theoretical *BER* performance for the ordinary QPSK receiver are shown. The theoretical performance of one receiver is plotted in order to illustrate the improvement for this case. The improvement to the performance seems to be approximately $9\ \text{dB}$ as measured from the plots. Perhaps this implies an improvement of

$$10\log_{10}\left(\frac{K}{2}\right)\text{dB}$$

in general. As previously, it is expected that theory and simulation results correspond for $BER > 10^{-5}$, because 10^6 symbols were generated.

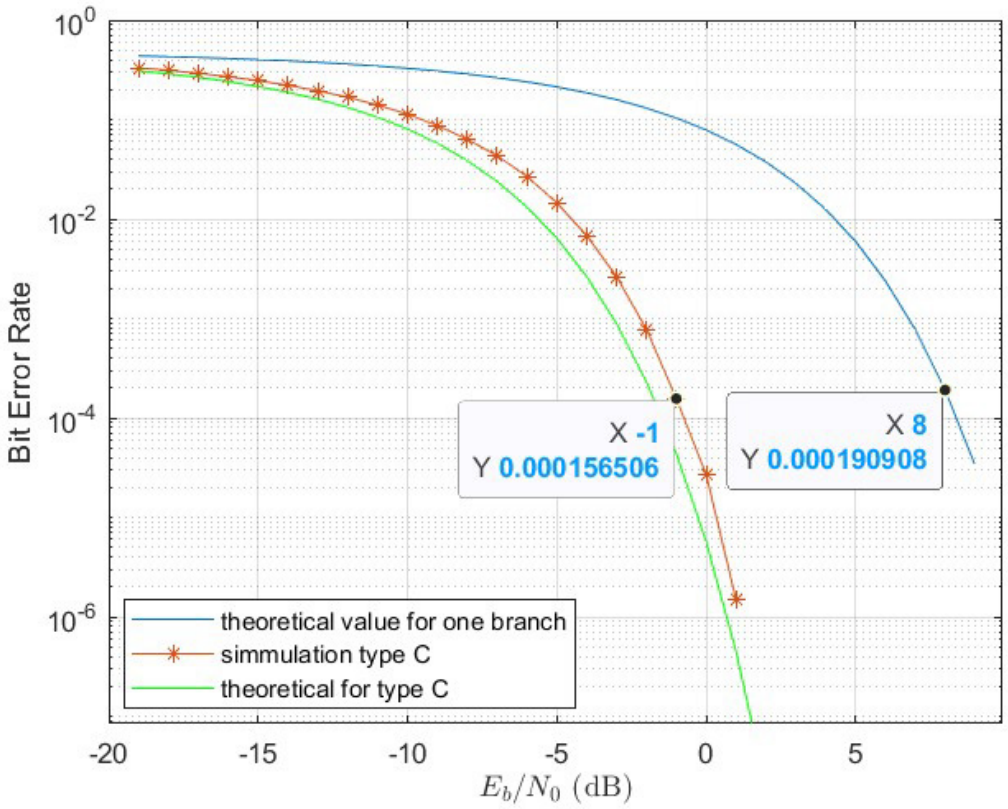

Figure 19. *BER* versus E_b/N_0 for super-receiver type-C for 15 branches

Based on the analysis and approximations in Chapter III, there is a noticeable discrepancy between the theoretical and simulated values. Despite this disparity, the two values appear to be close. It should be recalled that the analysis made some approximations, which are closest for large E_b/N_0. Consistent with this, we see from Figure 19 that for large E_b/N_0, the simulated and the analytical curves converge to within less than 1 dB, giving us confidence in the accuracy of the analysis and simulation.

V. CONCLUSION

In this final chapter of the thesis, a summary of the conducted research is presented, along with its key findings. Moreover, potential ways for further advancements and optimizations in the field of study are highlighted.

A. KEY FINDINGS

In Figure 20 and Figure 21, the *BER* curves for all the cases that were evaluated for this research are shown. The *BER* when five receivers are used and the *BER* when 15 receivers are used are shown in Figures 20 and 21 respectively. In both cases, 10^5 random symbols were generated.

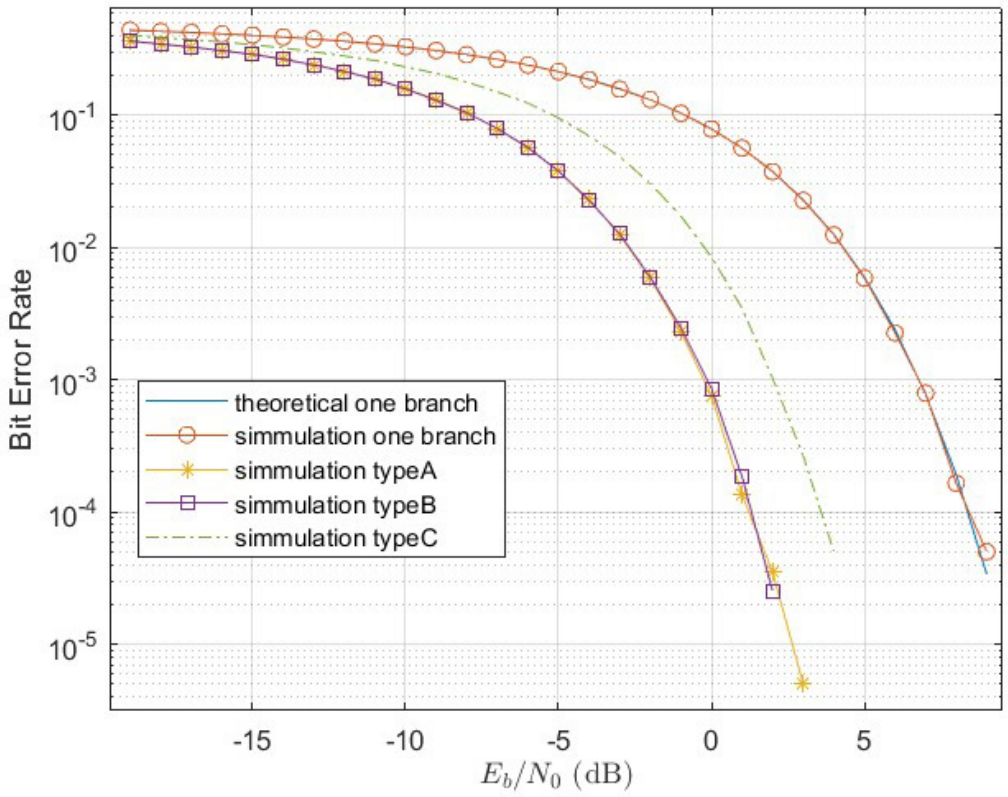

Figure 20. *BER* versus E_b/N_0 for five receivers

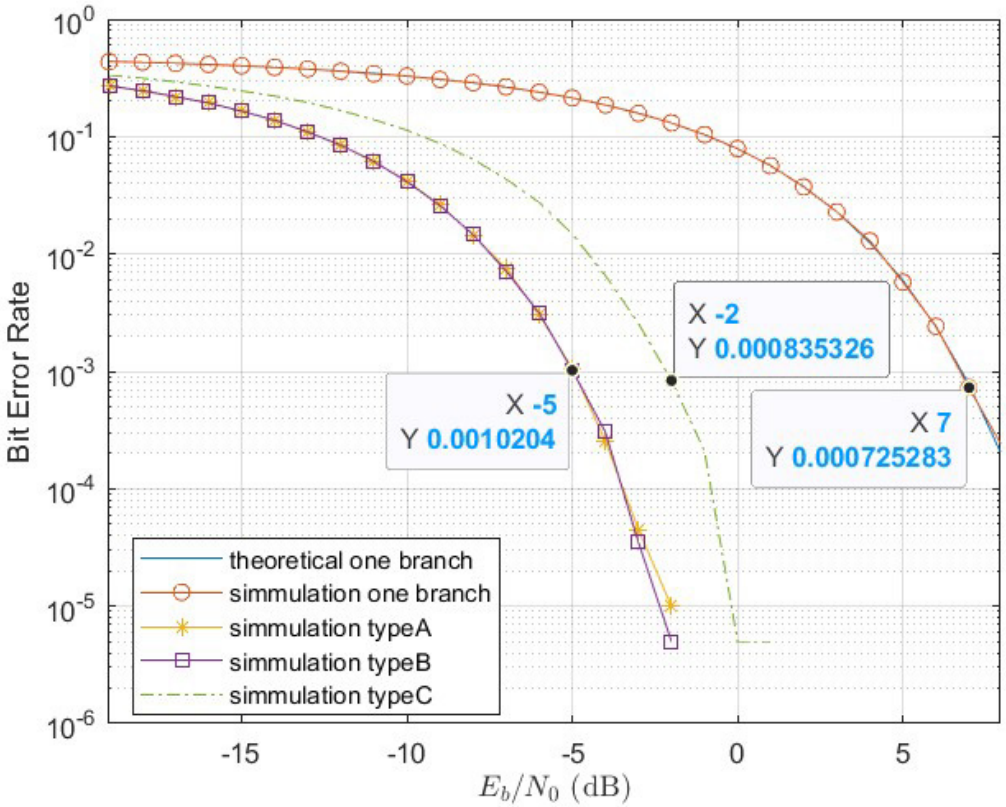

Figure 21. *BER* versus E_b/N_0 for 15 receivers

The curves in Figure 20 and Figure 21 illustrate that there is an improvement in the *BER* when multiple receivers are used as compared to the case of one receiver. Moreover, the more receivers that are used, the better the result. Considering the analysis in Chapter III, the improvement for each case can be calculated in advance. The improvement to the *BER* for super-receivers type-A and type-B is proportional to the total physical area of the antennas. On the other hand, the improvement for super-receiver type-C seems also to be proportional to the number of branches, but the improvement is roughly 3 dB less when measured by performance gain in dB.

Super-receiver type-A and type-B seem to have better *BER* performance compared to super-receiver type-C. In super-receiver types-A and -B, the noise from different branches is combined coherently before decisions are made. This allows positive and

negative noise values to combine to reduce noise. Super-receiver type-C does not combine noise in this way, and therefore, does not allow such noise reduction.

Another point that should be mentioned for this kind of communications system is the improvement in the distance of communications. As mentioned earlier in Section III.A, the total received power is increased by a factor of K for the first two types of receivers. That indicates that the distance of the communication could be increased by a factor of $\sqrt{K}$ and still have the same performance as in the case of one receiver. On the other hand, for the super-receiver type-C, the distance of communication could be increased by a factor of $\sqrt{K/2}$ and still have the same performance as the case of one receiver.

Finally, the idea that was originally proposed in this thesis seems to be feasible and brings about the desired result. *The desired result is to be able to have the sufficient probability of error for a very weak received signal*. This suggests that the initial estimate for construction of a system of multiple receivers that receive very weak signals such as in satellite communications seems to be feasible. The formation of an ad hoc larger array can improve the *BER* offering great advantages in communication systems.

B. FUTURE RESEARCH – RECOMMENDATIONS

The research on leveraging multiple receivers in digital communications is a promising field that should be further investigated. More studies should be done in this field.

One possible area for further exploration is the performance of these kinds of receivers when antennas with different characteristics are used. In our research, it was assumed that, for both the case of the one receiver and the multiple receivers, the antennas were identical. Further research could analyze the impact that the use of different sizes of antennas might have on the results. As shown, the improvement to the values of *BER* is proportional to the effective area of the antennas (Chapter III).

Additionally, further research should focus on the case that noise is introduced from the various parts of the receivers such as the LNAs. This case will differentiate super-receiver type-A from super-receiver type-B. In our research, we assumed that noise is

introduced only from the channel, but this is not the case in physical receivers. Every component through which the received signal passes adds noise, sometimes only slightly. Considering this, it is expected for super-receiver type-B to have inferior performance, since it uses *K* times more noisy parts (amplifiers, matched filters, etc.). This research needs to consider the nature of the actual components. For example, super-receiver type-A includes a noiseless component that adds together many low power RF signals. Future research would show if this would be a reasonable proposition or not, and how the results might be altered.

Furthermore, the ease of information transmission between the branches represents another crucial issue to consider when implementing these types of systems [5]. Combining the information before the LNA, as in the case of a super-receiver type-A, carries the risk of errors due to the very weak received signal at this point. Moreover, to ensure an accurate conversion of the analog signal to a digital signal for distribution among the branches, it is essential to sample and quantize the signal[9], however, this process is susceptible to even minor changes caused by noise, which can result in errors. The weakness of the signal at this stage increases the possibility of improper functioning of the analog-to-digital conversion (ADC) or of unacceptable quantization noise [9].

In contrast, for the super-receiver type-B, there is an improvement in the distribution among the branches because the received signal has been amplified before distribution. Similarly, the received signal in this case exhibits random values and requires multiple bits to represent each sample [9]. On the other hand, the super-receiver type-C presents a simpler distribution. Symbol decisions can be more easily transferred from one branch of the receiver to the final decision block, because each symbol can be represented by two bits. Future research could focus on exploring how to address and solve these challenges.

Finally, the effect timing and frequency synchronization might have on the employment of multiple receivers should be investigated. Considering the receivers are not in the same position and that it is possible they might move in different directions one from each other, the importance of synchronization is shown. If the timing and frequency of the transmitted and received signals are not synchronized, then combining the signals may not

be constructive, leading to a degraded signal quality. On the other hand, the possibility should be examined of introducing techniques where the branches work together, sharing information in the synchronization process.

THIS PAGE INTENTIONALLY LEFT BLANK

LIST OF REFERENCES

[1] A. Singh, M. R. Bhatnagar, and R. K. Mallik, "Cooperative spectrum sensing in multiple antenna based cognitive radio network using an improved energy detector," *IEEE Commun. Lett.*, vol. 16, no. 1, pp. 64–67, Jan. 2012 [Online]: Available: https://doi.org/10.1109/LCOMM.2011.103111.111884

[2] Y. V. Andreyev, "Multi-element system of ultra-wideband chaotic communications," *Syst. Signal Synchronization Gener. Process. Telecommun. SYNCHROINFO*, pp. 1–5, 2018 [Online]. Available: doi: 10.1109/ SYNCHROINFO.2018.8457024

[3] X. Chen, Z. Zhang, H.-H. Chen, and H. Zhang, "Enhancing wireless information and power transfer by exploiting multi-antenna techniques," *IEEE Commun Mag*, vol. 53, no. 4, pp. 133–141, Apr. 2015.

[4] E. Ochirsuren, L.S. Indrusiak, and M. Glesner, "An actor-oriented group mobility model for wireless ad hoc sensor networks," in *The 28th International Conference on Distributed Computing Systems Workshops*, Jun. 2008, pp. 174–179.

[5] T. C.-y Ng, W. Yu, J. Zhang, and A. Reid, "Joint optimization of relay strategies and resource allocations in cooperative cellular networks," presented at the *2006 40th Annual Conference on Information Sciences and Systems*, Princeton, NJ, USA, Mar. 2006, pp. 1553–1559 [Online]. Available: https://doi.org/10.1109/ CISS.2006.286386

[6] E. Webster, "MIMO (multiple input, multiple output)," *TechTarget*, Mar. 25, 2021 [Online]. Available: https://www.techtarget.com/searchmobilecomputing/ definition/MIMO

[7] B. Stewart, K. Barlee, D. Atkinson, and L. Crockett, *Software Defined Radio Using MATLAB Simulink and the RTL-SDR*, 1st ed. Glasgow, Scotland, UK: University of Strathclyde Engineering, 2015.

[8] B. Sediq and H. Yanikomeroglou, "Performance analysis of SNR-based selection combining and BER-based selection combining of signals with different modulation levels in cooperative communications," *IEEE 70th Veh. Technol. Conf. Fall Anchorage AK USA*, pp. 1–5, 2009 [Online]. Available: https://doi.org/ 10.1109/VETECF.2009.5378713

[9] B. Sklar, *Digital Communications – Fundamentals and Applications*, 2nd ed. Upper Saddle River, NJ, USA: Prentice Hall, 2011.

[10] M. Rice, *Digital Communications. A Discrete-Time Approach*, 1st ed. New York, NY, USA: Prentice Hall, 2008.

[11] T. T. Ha, *Theory and Design of Digital Communication Systems*, 1st ed. Cambridge, England, UK: Cambridge University Press, 2011.

[12] S. Miller and D. Childers, *Probability and Random Processes*, 2nd ed. Waltham, MA, USA: Academic Press, 2014.

INITIAL DISTRIBUTION LIST

1. Defense Technical Information Center
   Ft. Belvoir, Virginia

2. Dudley Knox Library
   Naval Postgraduate School
   Monterey, California